BIOCHEMISTRY
including biophysical chemistry & molecular biology

Article

pubs.acs.org/biochemistry

Pre-Steady-State Kinetic Characterization of Thiolate Anion Formation in Human Leukotriene C_4 Synthase

Agnes Rinaldo-Matthis,[†] Shabbir Ahmad,[†] Anders Wetterholm,[†] Peter Lachmann,[‡] Ralf Morgenstern,*[,§] and Jesper Z. Haeggström*[,†]

[†]Department of Medical Biochemistry and Biophysics (MBB), Karolinska Institutet, 171 77 Stockholm, Sweden

[‡]Department of Biochemistry and Biophysics, Stockholm University, 106 91 Stockholm, Sweden

[§]Institute of Environmental Medicine, Karolinska Institutet, 171 77 Stockholm, Sweden

ABSTRACT: Human leukotriene C_4 synthase (hLTC4S) is an integral membrane protein that catalyzes the committed step in the biosynthesis of cysteinyl-leukotrienes, i.e., formation of leukotriene C_4 (LTC_4). This molecule, together with its metabolites LTD_4 and LTE_4, induces inflammatory responses, particularly in asthma, and thus, the enzyme is an attractive drug target. During the catalytic cycle, glutathione (GSH) is activated by hLTC4S that forms a nucleophilic thiolate anion that will attack LTA_4, presumably according to an S_N2 reaction to form LTC_4. We observed that GSH thiolate anion formation is rapid and occurs at all three monomers of the homotrimer and is concomitant with stoichiometric release of protons to the medium. The pK_a (5.9) for enzyme-bound GSH thiol and the rate of thiolate formation were determined (k_{obs} = 200 s^{-1}). Taking advantage of a strong competitive inhibitor, glutathionesulfonic acid, shown here by crystallography to bind in the same location as GSH, we determined the overall dissociation constant (K_d^{GS} = 14.3 μM). The release of the thiolate was assessed using a GSH release experiment (1.3 s^{-1}). Taken together, these data establish that thiolate anion formation in hLTC4S is not the rate-limiting step for the overall reaction of LTC_4 production (k_{cat} = 26 s^{-1}), and compared to the related microsomal glutathione transferase 1, which displays very slow GSH thiolate anion formation and one-third of the sites reactivity, hLTC4S has evolved a different catalytic mechanism.

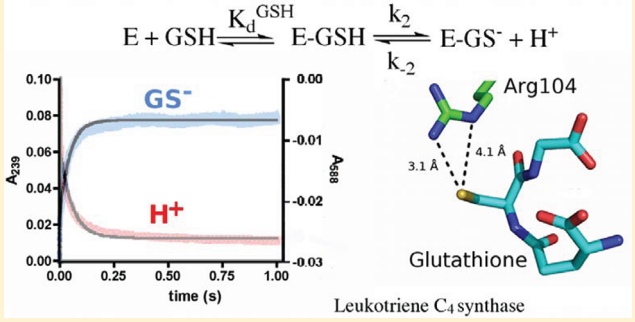

Cysteinyl-leukotrienes (cys-LT) LTC_4, LTD_4, and LTE_4 are mediators of allergy and anaphylaxis, provoking smooth muscle contraction and vascular responses. In the airways, the cys-LTs induce the cardinal signs of asthma: bronchoconstriction, mucus secretion, and edema formation.[1,2] The cys-LTs are formed from arachidonic acid in activated myeloid cells by sequential reactions catalyzed by 5-lipoxygenase, assisted by 5-lipoxygenase activating protein (FLAP), and leukotriene C_4 synthase (LTC4S).[3] Experimental and clinical data demonstrate the importance of cys-LTs in the pathophysiology of asthma, and specific drugs targeted against a cys-LT receptor constitute a commonly used new line of therapy against this disease.[4] However, many patients do not respond to these drugs, and therefore, there is a great need for more selective therapeutic agents.

The committed step in the formation of cys-LTs is the conversion of LTA_4 to LTC_4 through conjugation of the epoxide with reduced glutathione (Figure 1). The reaction is catalyzed by hLTC4S, which is a 17 kDa, integral membrane protein. hLTC4S belongs to a superfamily of homologous enzymes called MAPEG (membrane-associated proteins in eicosanoid and glutathione metabolism) that are all related to each other in primary (20−50% identical sequences), secondary, and tertiary structures.[5] The MAPEG superfamily has six human members. They are proteins involved in detoxification and in specific biosynthetic pathways of arachidonic acid metabolism. The six human members include FLAP and hLTC4S, involved in leukotriene biosynthesis;[1,6] microsomal glutathione *S*-transferase 1 (MGST1), MGST2, and MGST3, involved in detoxification; and microsomal prostaglandin PGE synthase 1 (mPGES-1), which catalyzes the oxidoreduction of PGH_2 to PGE_2.[7]

For efficient chemistry, GSH needs to be activated for its nucleophilicity to increase. This activation involves stabilization of the negatively charged thiolate anion. For hLTC4S, structural and biochemical evidence indicating that this stabilization is mediated via the positively charged Arg104 was recently presented.[8] Also in MGST1[9] and mPGES-1, the thiolate anion has been suggested to be stabilized by an arginine residue.[10,11] It is possible that all MAPEG members, except FLAP that lacks enzymatic function, use a similar mechanism for glutathione activation, prior to conjugation (or oxidoreduction) of their lipophilic substrates.

Received: September 6, 2011
Revised: December 15, 2011
Published: January 3, 2012

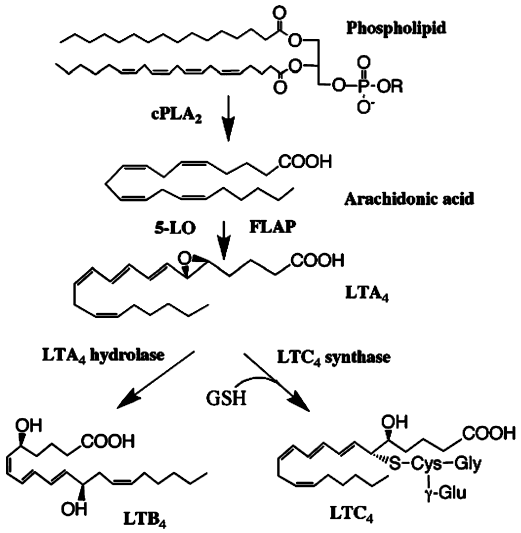

Figure 1. Schematic drawing of the leukotriene biosynthesis pathway where the function of hLTC4S is indicated.

The lipid substrate of hLTC4S, the fatty acid epoxide LTA_4, has been proposed to bind in a hydrophobic pocket close to the GSH binding site. hLTC4S is unusually selective for LTA_4, but it is very difficult to study direct binding because of the instability of the allylic epoxide in aqueous solution. Knowledge about binding and activation of substrates such as LTA_4 and GSH is required for understanding the chemical and catalytic mechanism of hLTC4S. In this study, we have focused on the first part of the reaction where GS^- (Scheme 1) is formed and a

Scheme 1

$$E + GSH \underset{k_{-1}}{\overset{k_1}{\rightleftharpoons}} E\text{-}GSH \underset{k_{-2}}{\overset{k_2}{\rightleftharpoons}} E\text{-}GS^- + H^+ \xrightarrow[LTA_4]{k_3} LTC_4$$

proton is released. We have determined the enzymatic binding affinity for GSH and GS^- and the kinetic parameters for the formation of the $E-GS^-$ species and its release (strictly speaking rate-limiting reprotonation). Because of its pivotal role in cys-LT biosynthesis, hLTC4S is an attractive drug target for the development of anti-inflammatory and anti-asthma drugs. Inasmuch as well-diffracting crystals of hLTC4S are now available,[8,13] this enzyme has also become amenable to structure-based drug design, and the success of this technique is strongly dependent on knowledge of the molecular mechanisms of catalysis, a major aim of this study.

MATERIALS AND METHODS

Chemicals. GSH and glutathione sulfonic acid (GSO_3^-) were from Sigma Aldrich. Bromocresol purple was from Fluka Chemie AG (Buchs, Switzerland), LTA_4 methyl ester from Cayman, and DDM from Anatrace. All other chemicals were obtained from common commercial sources. LTA_4 was produced by saponification of LTA_4 methyl ester with LiOH (6%, v/v) in tetrahydrofuran for 48 h at 4 °C.

Enzyme Preparation. Human LTC4S was expressed and purified from *Pichia pastoris* as previously described.[13] The protein used for pre-steady-state kinetic studies was purified without GSH using *S*-hexyl affinity chromatography, followed by a desalting step using a PD-10 column. The protein used for structural studies was purified in the presence of GSH using *S*-hexyl affinity chromatography and size exclusion chromatography. The protein concentrations were determined spectrophotometrically from the molar extinction coefficient ε_{280} of 27000 M^{-1} cm^{-1} of hLTC4S (M_r = 17 kDa) in addition to the Lowry method.[14] The proteins were concentrated using an Amicon centricon with a cutoff of 10 kDa, to 0.75 mg/mL for kinetic experiments and to 3 mg/mL for crystallization purposes.

Kinetics and Inhibition of Human LTC4S. During assays and determination of rate constants, three different buffers were used (buffers A–C). Buffer A consisted of 25 mM Tris (pH 7.8) and 0.03% Triton X-100. Buffer B consisted of 80 mM NaCl, 0.08 mM EDTA, 10% glycerol, 0.03% DDM, 5 mM β-mercaptoethanol (pH 7.0), and 20 μM bromocresol purple. Buffer C consisted of 20 mM Tris (pH 7.5), 5 mM β-mercaptoethanol, 100 mM NaCl, and 0.03% DDM. For the determination of proton release, the enzyme was subjected to buffer exchange using a PD-10 column, to buffer B for the determination of the rate of proton release and to the same buffer B without EDTA, glycerol, and bromocresol purple for the determination of the amount of proton released in a pH titration experiment.

The steady-state kinetic parameters of hLTC4S were determined in buffer A at an assay temperature of 20 °C in 100 μL incubation mixtures with 0.2 μg of enzyme. To determine kinetic parameters V_{max} and K_m of LTA_4, the substrate LTA_4 concentration was varied between 3 and 66 μM and the GSH concentration was kept constant at 2 mM. Triplicate or duplicate determinations were performed for each condition. The reaction mixtures were incubated for 15 s, and formation of the LTC_4 product was assessed using high-performance liquid chromatography (HPLC) as described previously.[8] The Michaelis–Menten parameters K_m and V_{max} were determined by plotting the velocity of LTC_4 product formation versus the substrate LTA_4 concentration and fitting the plotted values to the Michaelis–Menten equation for steady-state kinetics (Table 1).

The inhibition constant (K_i) for GSO_3^- binding to hLTC4S was measured using the assay described above where reaction mixtures contained constant levels of LTA_4 (30 μM), varied amounts of GSH (0.05–5 mM), six different concentrations of GSO_3^- (0–600 μM), and 0.2 μg of enzyme in buffer A. The reaction mixtures were preincubated with GSO_3^- for 45 s followed by incubation for 30 s with 30 μM LTA_4 and 0.05–5 mM GSH prior to the addition of 200 μL of MeOH. Quantification of the amount of LTC_4 produced was performed using HPLC as described previously.[8] The mode of inhibition was studied using Lineweaver–Burk plots (data not shown), and the K_i value was obtained by fitting the data to the extended Michaelis–Menten equation for competitive inhibition using GraphPad Prism.

Table 1. Steady-State Kinetic Parameters of hLTC4S

substrate	K_m (mM)	V_{max} (μmol min^{-1} mg^{-1})	k_{cat} (s^{-1})	k_{cat}/K_m (M^{-1} s^{-1})
GSH[a]	0.3 ± 0.06	35 ± 2	12 ± 0.7	(4 ± 1.1) × 10^4
LTA_4	0.03 ± 0.01	78 ± 12	26 ± 4	(8.7 ± 4) × 10^5

[a]Data from ref 8.

dx.doi.org/10.1021/bi201402s | *Biochemistry* 2012, 51, 848–856

Stopped-Flow Experiments. An Applied Photophysics stopped-flow instrument equipped with either one or two monochromators was used for all experiments; 55 μL from each of two syringes was rapidly mixed in the 10 mm path length cell if not otherwise indicated, and the signal was recorded. In general, three to six trace averages were used to fit theoretical expressions describing single exponentials. All experiments were performed at 20 °C, and the concentrations given below are the resulting concentrations in the mixing chamber.

To determine the pK_a of the enzyme−GSH thiolate, we measured thiolate anion formation using stopped-flow measurements at varying pH values. The enzyme (20 μM, mixing chamber), in buffer C, was rapidly mixed with the same buffer C that had an increased buffer capacity of 100 mM at pH 5.5−8.5 with the addition of 0.5 mM GSH (mixing chamber); 100 mM sodium phosphate buffer was used to buffer the pH between 5.5 and 7.0, and 100 mM Tris was used as a buffer for measurements at pH 7−8.5. We tested both buffers with 0.5 mM GSH at pH 7 to be certain there was no GSH binding difference because of the buffer used. For each pH, five to seven measurements were recorded and the amplitude at 239 nm, corresponding to the amount of thiolate formed ($\epsilon_{\text{thiolate anion}}$ = 5000 M^{-1} cm^{-1}), was plotted versus pH (Figure 2). The pK_a was determined by fitting the data to the equation pK_a = max amplitude/(1 + $10^{-pH}/K_a$) in GraphPad Prism.

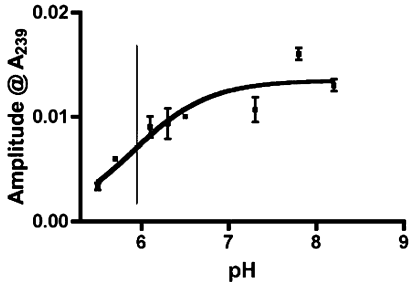

Figure 2. pK_a of thiolate anion formation in hLTC4S determined by measuring the amount of thiolate anion formed (the amplitude) at 239 nm (y-axis) at different pH values (x-axis) using stopped-flow measurements. The pK_a of 5.9 was determined by fitting the experimental data to the equation pK_a = max amplitude/(1 + $10^{-pH}/K_a$).

The velocity of thiolate anion formation was studied using a stopped-flow experiment in which the enzyme in buffer C was rapidly mixed with the same buffer containing increasing concentrations of GSH (from 0.05 to 5 mM). The appearance of absorbance at 239 nm was followed and fitted to the single-exponential equation $Y = A\exp(-k_{obs}t) + C$ with GraphPad Prism, where Y is the absorbance, A is the amplitude, k_{obs} is the observed rate, and C is the end point of the signal. The observed rates of thiolate anion formed were plotted (y-axes) at each GSH concentration (x-axes). The plotted k_{obs} values were fitted to eq 1

$$k_{obs} = k_{-2} + \frac{k_2[GSH]}{K_d^{GSH} + [GSH]} \quad (1)$$

which describes a two-step mechanism involving the formation of a rapid equilibrium of an initial E−GSH complex (see Scheme 1), and we could calculate, using GraphPad Prism, the equilibrium dissociation constant K_d^{GSH} and rate constants k_2 and k_{-2}. To obtain a more accurate value of k_{-2}, we performed a GSH release experiment in which the rate of release of GSH from the enzyme−GSH complex was determined by the rapid dilution of a mixture of hLTC4S (20 μM, mixing chamber) in equilibrium with a nonsaturating amount of GSH (15 μM, mixing chamber) in buffer C. The release of GSH was followed by the loss of absorbance at 239 nm upon dilution with the same amount of buffer solution. The rate was obtained by fitting a single-exponential function with an averaged (four traces) progression curve using Pro-data SX software provided with the stopped-flow apparatus.

The dissociation constant of the thiolate anion ($K_d^{GS^-}$) was obtained from an experiment in which the GSH release was followed at 239 nm by mixing 20 μM purified enzyme (mixing chamber) containing 1, 5, 10, 25, 50, and 100 μM GSH in buffer C with 2 mM GSO_3^- (mixing chamber) in the same buffer. The amplitude of the thiolate signal as well as the rate of thiolate release was recorded at 239 nm. The amplitude for thiolate at 239 nm (y-axes = bound GSH) was measured at each concentration of GSH (x-axes = free GSH). The amount of thiolate was calculated using ϵ(thiolate anion) = 5000 M^{-1} cm^{-1}. The $K_d^{GS^-}$ could be obtained by fitting the data to a one-site binding hyperbolic equation (eq 2) in GraphPad Prism

$$[\text{bound } GS^-] = \frac{B_{max}[\text{free GSH}]}{K_d^{GS^-} + [\text{free GSH}]} \quad (2)$$

where B_{max} is the maximal amount of GS^- bound and $K_d^{GS^-}$ is the concentration of ligand required to reach half-maximal GS^- binding. To be sure that we could use GSO_3^- as a tool to determine $K_d^{GS^-}$, we determined the mode of inhibition and affinity of GSO_3^- prior to the actual GSH release experiment (see above).

To measure the rate of proton release, we used stopped-flow experiment in which the enzyme (20 μM, mixing chamber) was mixed with 0.5 mM GSH (mixing chamber) in buffer B (pH 7.0). The change in pH was followed as an absorbance decrease using the pH sensitive dye bromocresol purple at 588 nm. To correct for dye fluctuations, we conducted a control experiment using the same conditions described above without the enzyme (data not shown).

Potentiometric Measurements. To determine the stoichiometry of GSH thiolate binding, we measured the amount of proton released per amount of enzyme using a pH meter (PHM210, MeterLAB). The enzyme (80 μM), in buffer B without bromocresol purple, glycerol, and EDTA, at pH 7.45, 7.48, and 7.45, was mixed with 1 mM GSH (in the same buffer at the same pH). The pH change was measured using a pH meter under a continuous nitrogen flow. Finally, 70, 80, and 70 μM NaOH were used to titrate the solutions back to the original pH values of 7.45, 7.48, and 7.45, respectively.

Crystallization of the hLTC4S−GSO_3^- Complex. Crystals of hLTC4S were grown and cryo-cooled as described in ref 13. To obtain the hLTC4S−GSO_3^- complex, the crystals were soaked for 1 h in a solution of mother liquor supplemented with 1 mM GSO_3^- prior to being transferred to a cryo-solution.

Data Collection. Diffraction data were collected to a resolution of 2.9 Å using a wavelength of 0.8726 Å for the complex at 100 K on beamline ID23-2 at the European Synchrotron Radiation Facility (ESRF) using a CCD 225 mm MarMOSAIC detector. Each frame was exposed for 1 s with an oscillation range of 1°. The XDS package[15] was used for indexing and integration. Scaling of the data was done using SCALA[16] in the CCP4 suite;[17] for statistics, see Table 2.

Determination and Refinement of Structure. The native hLTC4S structure [Protein Data Bank (PDB) entry

Table 2. Data Collection and Refinement Statistics[a] for the Crystal Structure of hLTC4S in Complex with GSO_3^-

Data Collection	
space group	*F*23
cell dimensions	
a, *b*, *c* (Å)	170, 170, 170
α, *β*, *γ* (deg)	90, 90, 90
resolution (Å)	2.9 (3–2.9)
R_{sym} or R_{merge}	14.5 (85.5)
R_{pim}	0.029 (0.17)
$I/\sigma I$	26 (5.2)
completeness (%)	99.9 (100)
redundancy	25.1 (25.4)
Refinement	
resolution (Å)	2.9
no. of reflections	9259
R_{work}/R_{free}	18/23
no. of atoms	
protein	1135
ligand/ion	9
water	87
B factor	
protein	45
ligands	43
water	48
root-mean-square deviation	
bond lengths (Å)	0.015
bond angles (deg)	1.582

[a]Values in parentheses are for the highest-resolution shell.

2uuh] without ligands or waters was used for initial rigid body refinement of the data for the hLTC4S–GSO_3^- complex. The $F_o - F_c$ maps produced showed clear electron density representing the GSO_3^- inhibitor. REFMAC5[18] in the CCP4i package was used for refinement of coordinates and *B* factors. COOT[19] was used for molecular modeling. For refinement and data collection statistics, see Table 2. The model of the GSO_3^- inhibitor was obtained from the PDB, and REFMAC5 was used to generate a library for the GSO_3^- inhibitor. The GSO_3^- molecule was built into the density shown in the active site corresponding to the bound GSO_3^-. All figures were made using PYMOL (DeLano Scientific).

The coordinates and structure factors for the hLTC4S–GSO_3^- complex were deposited in the PDB as entry 3HKK.

RESULTS

Steady-State Kinetics. To obtain steady-state kinetic parameters, we performed conventional initial rate measurements (Table 1). The V_{max} and K_m for GSH were described and published previously,[8] and here we determined V_{max} and K_m for LTA_4. $K_m^{LTA_4}$ was 30 ± 10 μM, and $V_{max}^{LTA_4}$ was 78 ± 12 μmol min^{-1} mg^{-1} (n = 3). The corresponding k_{cat} for LTA_4 is 26 s^{-1}, and the k_{cat} for GSH is 12 s^{-1}. The lower value of k_{cat} for GSH is due to the lower solubility and stability of LTA_4 compared with those of GSH. The inhibition pattern of GSO_3^- when the GSH concentration was varied indicated competitive inhibition toward GSH, and the K_i for GSO_3^- toward hLTC4S was calculated to be 26 ± 6 μM (n = 3) (data not shown).

Thiolate Anion Formation in hLTC4S. It has been suggested that hLTC4S stabilizes a GS^- thiolate[13] as an important part of chemical catalysis. In a previous study, we found direct evidence of the formation of this molecular species by UV difference spectroscopy.[8] The amplitude of the thiolate spectrum obtained[8] corresponded to a GS^-:hLTC4S monomer stoichiometry of 1:1, indicating that all three active sites in the hLTC4S trimer are catalytically competent. The fact that the thiolate is formed by hLTC4S at pH 7.5 demonstrates that the enzyme can lower the pK_a of the GSH, which is usually around 8–9 in solution.[20] To determine the pK_a of the enzyme-bound GSH, we measured the amplitude of GS^- formation using stopped-flow measurements at pH values ranging from 5.5 to 8.5. hLTC4S displayed a pK_a of 5.9 for the enzyme-bound GSH (Figure 2).

To obtain the microscopic rate constant for the formation of GS^-, pre-steady-state kinetics using a stopped-flow experiment was determined. Mixing hLTC4S with GSH, as presented here, resulted in a rapid increase in absorbance at 239 nm reflecting formation of the reactive GS^- (Figure 3A). We were not able to obtain accurate data at GSH concentrations of >5 mM, because of the fast formation of GS^- approaching the instrument dead time. The amplitude of the measured absorbance signal was 0.09, which corresponds to a stoichiometry of 0.9 GS^- formed per monomeric enzyme using an $\varepsilon_{thiolate\ anion}$ of 5000 M^{-1} cm^{-1}. The observed apparent first-order rate constants, k_{obs}, at different GSH concentrations were fit to eq 1 and exhibited a hyperbolic dependence on substrate concentration (Figure 3B). The saturation behavior is consistent with a two-step

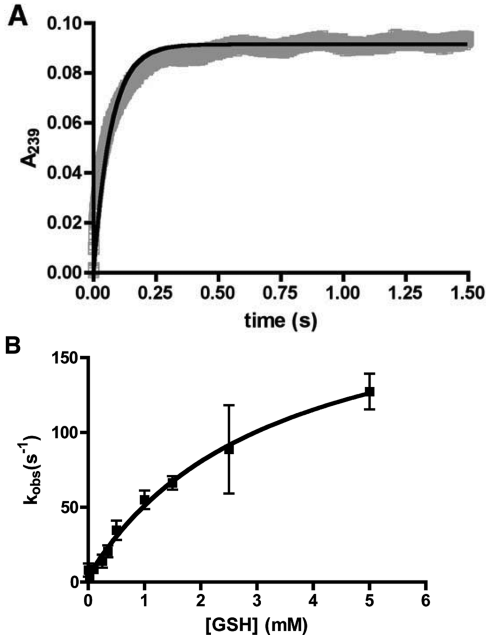

Figure 3. Determination of the rate of thiolate anion formation in hLTC4S. (A) Representative example of stopped-flow experimental data (gray) of thiolate anion formation as observed at 239 nm when mixing 20 μM hLTC4S (mixing chamber) with 0.5 mM GSH (mixing chamber). The black line is a fit of the experimental data to a single exponential with a k_{obs} of 14.3 s^{-1}. Thiolate formation causes an increase in absorbance at 239 nm of ~0.09 with a $t_{1/2}$ of 0.05 s. The observed amplitude corresponds to a stoichiometry of 0.9 per monomeric protein. (B) Dependence of k_{obs} on the concentration of GSH where different k_{obs} rates from panel A were fitted to eq 1 and the saturation of the curve shows a k_{obs} or k_2 value of 200 ± 26 s^{-1} and a K_d^{GSH} of 3 ± 0.6 mM. Four to six measurements were performed at each GSH concentration.

dx.doi.org/10.1021/bi201402s | *Biochemistry* 2012, 51, 848–856

mechanism,[12] involving a rapid equilibrium formation of an initial E−GSH complex ($K_d^{GSH} = k_{-1}/k_1 = 3.0 \pm 0.6$ mM), followed by the E−GS$^-$ complex formed with a rate constant k_2 of 200 ± 26 s^{-1} ($n = 4$). The rate of thiolate protonation (k_{-2}) could not be determined accurately from these fits but was conveniently obtained by measuring the rate of release of GSH from the E−GS$^-$ complex using a GSH release experiment.

GSH Release Experiment. The rate of release of GSH from the enzyme thiolate complex was studied using the stopped-flow method by rapid dilution of a mixture of hLTC4S in equilibrium with a nonsaturating amount of GSH.[21] The release of GSH was followed by the loss of absorbance at 239 nm upon dilution with the same amount of buffer solution. The first-order rate constant k_{-2} for GSH release was 1.3 ± 0.006 s^{-1} (Figure 4).

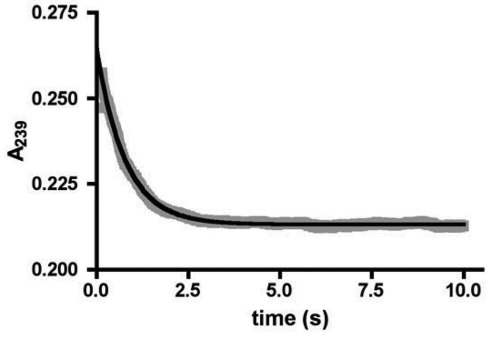

Figure 4. Determination of the k_{-2} rate constant in which experimental data from a representative GSH release experiment are shown as observed at 239 nm where a solution of 20 μM hLTC4S (mixing chamber) and a nonsaturating amount of 15 μM GSH (mixing chamber) in buffer C was rapidly mixed with the same amount of buffer C solution. The k_{-2} of 1.3 ± 0.006 s^{-1} was obtained by fitting the experimental data from six measurements (gray) to a single-exponential equation (black line).

Dissociation Constant for GS$^-$ ($K_d^{GS^-}$). To determine the constant for dissociation of GS$^-$ from hLTC4S, we used the GSH release competition experiment in which the enzyme was allowed to equilibrate with varying GSH concentrations and then rapidly mixed with an excess of the competitive inhibitor GSO_3^- and the decrease in the magnitude of the GS$^-$ signal was observed at 239 nm. Figure 5A shows a representative example of a signal obtained when mixing enzyme and GSH with GSO_3^-, with concentrations of 20 μM, 50 μM, and 2 mM, respectively, in the mixing chamber. The resulting amplitude in Figure 5A is 0.097, which is close to a stoichiometry of one GS$^-$ formed per monomeric protein. To obtain the $K_d^{GS^-}$, several measurements were performed using concentrations of enzyme, GSH, and GSO_3^- of 20 μM, 1−100 μM, and 2 mM, respectively, in the mixing chamber. The amplitude, representing bound GS$^-$ in the thiolate form, was plotted versus the amount of free GSH (Figure 5B). Four to six traces were recorded for each GSH concentration, and the data originate from two independent experiments. When the data were fit to eq 2 using GraphPad Prism, we obtained an apparent dissociation constant $K_d^{GS^-}$ of 14.3 ± 2.4 μM.

Proton Release. When GSH is deprotonated to form the nucleophilic GS$^-$, the proton can be either taken up by a residue on the protein or released to the solvent. Using bromocresol purple as a pH indicator, we measured the rate of proton release during GS$^-$ formation at 588 nm using stopped-flow analysis (Figure 6). The rate of release of proton into the solvent matched the rate of GS$^-$ formation (Figure 3A). With bromocresol purple, we were not able to quantify the amount of proton released. To quantify the amount of proton released, we conducted potentiometric titration experiments ($n = 3$), and the concentration of NaOH used to titrate back to the original pH was similar (70, 80, and 70 μM) to the concentration of

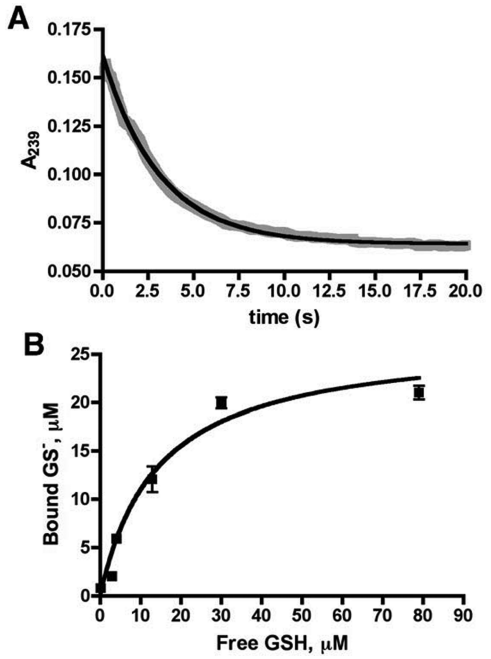

Figure 5. Determination of the constant for dissociation of GS$^-$ ($K_d^{GS^-}$) from hLTC4S. (A) Experimental data from a representative GSH release competition experiment as observed at 239 nm where a solution of hLTC4S and GSH in buffer C was rapidly mixed with GSO_3^- (buffer C), where the concentrations of the reactants were 20 μM, 50 μM, and 2 mM, respectively, in the mixing chamber. The amplitude of 0.097 corresponds to a stoichiometry of one GS$^-$ formed per monomeric protein. (B) The $K_d^{GS^-}$ of 14.3 ± 2.4 μM was obtained by fitting the recorded amplitudes from several GSH release competition experiments to eq 2. Each data point represents an average from four to six measurements from two different experiments.

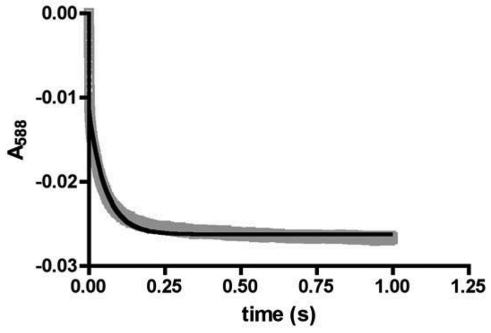

Figure 6. Rate of proton release measured with a pH sensitive dye at 588 nm when mixing hLTC4S (20 μM) with 0.5 mM GSH. The experimental data from the proton release experiment are colored gray, and the black line is a fit of the experimental data to a single exponential with a k_{obs} of 18 s^{-1}. The proton release yields an absorbance decrease of ~0.015, and this process has a $t_{1/2}$ of 0.03 s.

enzyme used (80 μM monomer), which suggests that one GS^- is formed per protein monomer.

Crystal Structure of hLTC4S with GSO_3^-. The structure of hLTC4S in complex with GSO_3^- was determined to 2.9 Å resolution by X-ray crystallography so we could understand inhibitor binding in a structural context. The competitive inhibitor binds with full occupancy in the active site of the protein, and the $F_o - F_c$ maps that were produced showed clear electron density contoured at 3σ representing the GSO_3^- inhibitor (Figure 7A). The atomic model contains residues 1−150 for the monomeric form of trimeric hLTC4S. The largest part of the N-terminal His_6 tag (residues −6 to −1) and the last C-terminal residue were not built into the model because of the lack of electron density. The residues of the atomic model show good agreement with the observed diffraction data and expected bond lengths and bond angles. The majority of the residues (98.6%) are located in the allowed region in the Ramachandran plot,[22] and the two residues that were outliers are located on a loop region on the surface of the protein, not considered to be important for catalysis. The structure of the hLTC4S monomer is highly similar to that of the native enzyme with rmsds of 0.23 Å in the backbone α-carbons, and with only small differences in the active site. Upon comparison of the active sites of the GSO_3^- complex and the GSH-containing structure (PDB entry 2uuh), Arg104 has shifted its position slightly, making a closer contact with the sulfonic acid part of GSO_3^- compared with the SH group (strictly speaking thiolate) in the GSH complex (Figure 7B,C).

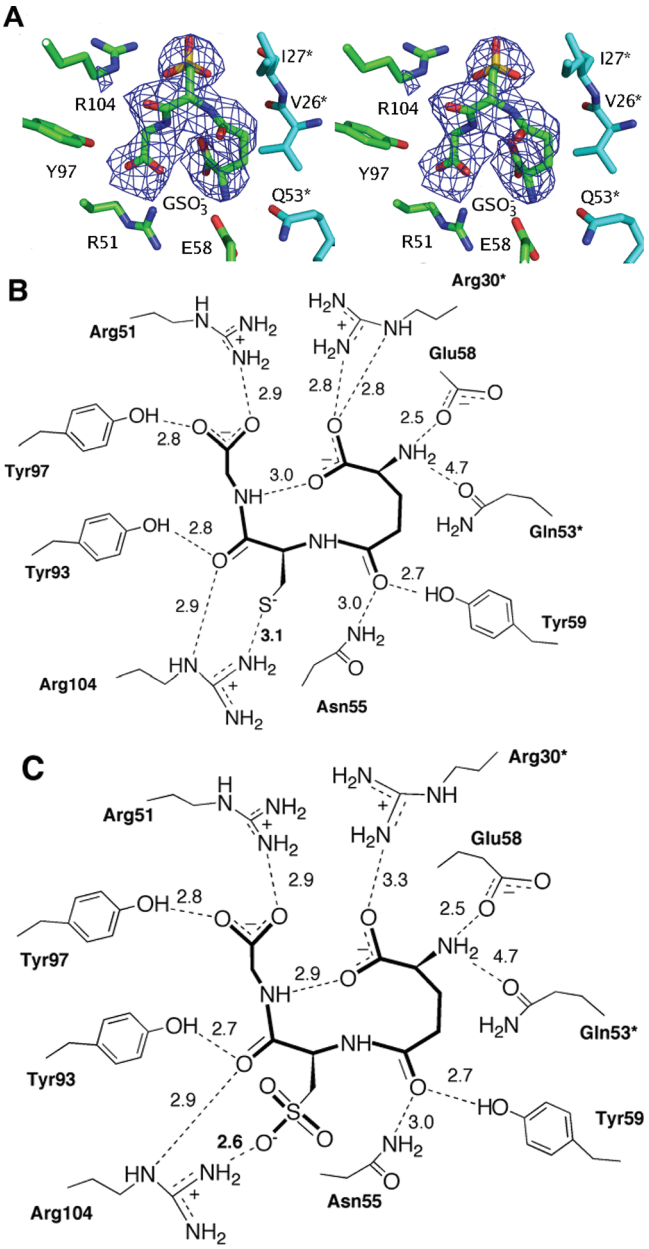

Figure 7. (A) Stereoview of the active site of hLTC4S in complex with GSO_3^- where the electron density is colored green and was calculated from an $F_o - F_c$ map contoured at 3σ. Asterisks denote residues from the neighboring monomer. (B and C) Schematic drawing of GSH (B) from PDB entry 2uuh and GSO_3^- (C) interactions in the active site of hLTC4S. The numbers correspond to distances in angstroms. Note that the distances between Arg104 and the oxygen from GSO_3^- and the sulfur from GSH differ in the two structures.

DISCUSSION

A central theme for many GSH-dependent enzymes is deprotonation of glutathione to form the highly reactive GS^- at physiological pH.[20,23] This property was suggested for hLTC4S,[13,24] and we were recently able to experimentally show that hLTC4S is able to form a thiolate using UV difference spectra.[8] Enzymes that use a thiolate anion as a nucleophile in their catalytic reaction have the ability to reduce the pK_a of GSH. We used pre-steady-state stopped-flow kinetics to determine the pK_a of GS^- formation in hLTC4S. The amplitude at 239 nm, corresponding to the amount of GS^- formed, was recorded at different pH values. We found that hLTC4S lowers the pK_a of enzyme bound GSH to 5.9 (Figure 2). This value is in the range of those seen for most glutathione transferases (pK_a = 6−7)[20,23,25] probably because further reduction of the pK_a gives only marginal increases in the proportion of thiolate at physiological pH.

We used pre-steady-state kinetics to further analyze the kinetic properties of GS^- activation in hLTC4S. Analysis of GS^- formation gives good estimates for the maximal GS^- formation rate (k_2) and binding of GSH (K_d^{GSH}) before deprotonation. In contrast to another structurally related member of the MAPEG superfamily, MGST1, hLTC4S catalyzes a rapid formation of GS^- (k_2 = 200 s^{-1}) (Figure 3A,B). Furthermore, the amount of GS^- formed and the amount of protons released were stoichiometric, as seen from UV difference spectra,[8] potentiometric measurements, and stopped-flow experiments, suggesting one GS^- per active site of hLTC4S, again in contrast to MGST1 that displays one-third of the sites reactivity only stabilizing one GS^- per trimer.[26]

Upon comparison of the $k_{cat}^{LTA_4}$ (26 s^{-1}) for hLTC4S with GS^- formation (k_2 = 200 s^{-1}), it is clear that GS^- formation is not a rate-limiting step for the overall reaction as seems to be the case for MGST1 with reactive xenobiotic substrates.[27] These properties of hLTC4S indicate that the enzyme, being substrate specific, has evolved an efficient catalysis imperative for physiological turnover of the highly unstable LTA_4. The k_{cat}/K_m value (Table 1) for LTA_4 of 8.7 × 10^5 M^{-1} s^{-1} and use of all three active sites further support this suggestion.

To further analyze binding of GSH to hLTC4S, we determined the release or the off rate of GS^- (Figure 4) using a GSH release experiment. This process is slow (1.3 s^{-1}) and occurs on a convenient time scale yielding very robust data of k_{-2} that fit a single exponential.

dx.doi.org/10.1021/bi201402s | Biochemistry 2012, 51, 848−856

To obtain the apparent binding affinity constant ($K_d^{GS^-}$) of the thiolate toward hLTC4S (Table 3), the competitive inhibitor GSO_3^- was used in the stopped-flow kinetic

Table 3. Microscopic Rate Constants and Affinity Constants for Binding of GSH and GS^- to hLTC4S

K_d^{GSH}	3.0 ± 0.6 mM
k_2	200 ± 26 s^{-1}
k_{-2}	1.3 ± 0.006 s^{-1}
$K_d^{GS^-}$	14.3 ± 2.4 μM

experiment (Figure 5A,B). Prior to using GSO_3^- as an experimental tool, we characterized the inhibition constant and mode of inhibition of GSO_3^- toward hLTC4S using inhibition steady-state kinetics. The competitive mode of binding was confirmed by determining the crystal structure of hLTC4S in complex with GSO_3^-, revealing that GSO_3^- binds to the hLTC4S active site in the same place as GSH in the previously determined structure (PDB entry 2uuh). The observed competitive mode of binding and the relatively high affinity of GSO_3^- for hLTC4S (K_i = 26 μM) allowed us to feel confident in using GSO_3^- as a tool to measure the $K_d^{GS^-}$. The $K_d^{GS^-}$ was found to be 14.3 μM, which is ≥200 times tighter than that for the protonated GSH (K_d^{GSH} = 3 mM). If GSH binding and thiolate formation both were in "rapid" equilibrium during steady-state turnover (chemistry being slow), one would expect a K_m for GSH ≈ $K_d^{GS^-}$. As the K_m is considerably higher (K_m^{GSH} = 0.3 mM), it suggests that chemistry is rapid enough to decrease the amount of thiolate anion species during steady-state turnover so that the GSH−enzyme interaction contributes to K_m. In other words, the resulting so-called Briggs−Haldane kinetics ($K_d < K_m$) is one hallmark of efficient catalysis.[28]

The rate of GS^- release, the rate of GS^- formation, and the GSH and GS^- affinity constants all together make a complete description of the GSH−enzyme interaction, and we can now also calculate the composite macroscopic $K_d^{GS^-}$ for GSH using eq 3. The calculated value of $K_d^{GS^-}$ is 19 ± 0.01 μM using eq 3 with the observed constants as input values: k_2 = 200 s^{-1}, k_{-2} = 1.3 s^{-1}, and K_d^{GSH} = 3.0 mM. This value is in good agreement with the measured $K_d^{GS^-}$ of 14.3 ± 2.4 μM.

$$K_d^{GS^-} = \frac{[E][GSH]}{[E-GSH]\left(1 + \frac{k_2}{k_{-2}}\right)} \text{ and}$$

$$K_d^{GSH} = \frac{[E][GSH]}{[E-GSH]} \text{ we get}$$

$$K_d^{GS^-} = \frac{K_d^{GSH}}{1 + \frac{k_2}{k_{-2}}} \quad (3)$$

Many studies have been performed to determine the mechanism behind deprotonation of the GSH in soluble glutathione transferases. Some studies discuss base-assisted deprotonation[29] through a residue in the protein or through the carboxylate moiety of GSH.[30] Other studies indicate the importance of an active site water assisting the deprotonation.[31] Duorado et al.[32] discuss a scenario in which a combination of the three mechanisms described above would occur simultaneously to activate the thiol. In the soluble GST classes, alpha, mu, and pi, there is a conserved Tyr thought to stabilize the thiolate, and members of the soluble GST classes, theta and delta, have a Ser involved in stabilization of the thiol.[23] An Arg residue in concert with a Tyr has been shown to stabilize the thiolate in the mu subclass, hGSTM2,[33] and in the alpha GSTA1-A1.[34] In these GSTs, the Arg is suggested to work in concert with a catalytically important Tyr. In hLTC4S, both the structure and kinetic data show that an Arg residue alone is responsible for formation of the thiol. Probably, thiolate formation in hLTC4S is assisted by electrostatic stabilization by the positively charged Arg104. The fact that the Cys thiolate of GSH is not juxtaposed to any other basic residue as well as the high pK_a of 12 for Arg residues suggests that the thiolate is formed through the direct release of a proton to solvent (via coordinated water). To study the rate of release of a proton in hLTC4S, we used stopped-flow kinetics using the pH sensitive dye bromocresol purple. We could record at 588 nm a rapid decrease in pH corresponding to proton release during thiolate anion formation. The processes of proton release and thiolate anion formation using the same amount of protein and GSH have similar k_{obs} values of 18 and 14 s^{-1}, respectively, which suggest that the proton released originates from GSH (Figure 6). In this study, we did not investigate possible protonation events during the actual conjugation reaction between LTA_4 and GSH. Previous studies[24] have discussed a scenario in which the thiol proton would be shuttled to the oxygen at C5 of LTA_4 to assist in oxyanion protonation. From this investigation, proton shuttling in the conjugation reaction cannot be ruled out because our study was limited to the first part of the reaction. The proton transfer would probably not be rate-limiting.

To understand how GSO_3^- is bound to hLTC4S, we determined the crystal structure of hLTC4S in complex with GSO_3^- to a resolution of 2.9 Å. In a recent study by Armstrong and co-workers on MPGES1,[35] GSO_3^- was seen to result in different H/D dynamics compared to those with GS^-. In this study, the GSO_3^- is bound in the same horseshoe shape (Figure 7A) that is seen for GS^- in PDB entry 2uuh.[13] This bent shape differs from the way in which GS^- and GSO_3^- are bound in soluble dimeric GSTs where they adopt an extended conformation.[23,36] The bent GSO_3^- molecule allows for dual interactions with Arg104 via both NH2 and NH1 (Figure 7B,C). Upon examination of hydrogen bond interactions between Arg104 and the GSO_3^- moiety, one significant difference from the GS^- complex can be observed. Arg104 makes a stronger interaction with the oxygen atom of GSO_3^- as compared with the sulfur in the GSH−hLTC4S complex (Figure 7B,C).

Interestingly, the DDM molecule that can be seen in PDB entry 2uuh is not present in the GSO_3^- complex. One reason for this observation could be that the more bulky sulfate part is situated in a way that hinders the DDM from binding. This might indicate that very precise interactions between the GSH-bound enzyme form and LTA_4 are required for efficient substrate binding, consistent with the high substrate selectivity and efficiency of hLTC4S. Hence, GSH binding could be an important contributor to the specificity toward LTA_4, a notion that would mean an ordered kinetic mechanism rather than a random mechanism as previously suggested.[37]

In summary, these studies reveal that hLTC4S displays rapid GSH thiolate formation (k_2 = 200 s^{-1}), suggesting that, in the cell, a thiolate anion is bound to the protein at all times and, therefore, a thiolate-bound form of hLTC4S might be a suitable model of choice to consider for structure-based drug design. The thiolate anion of GSH is stabilized by Arg104, which provides a favorable electrostatic field allowing for dissociation of the proton. This proton is released to solvent water at a rate that is the same as the rate of thiolate anion formation. The lack of bound detergent mimicking LTA_4 in the hLTC4S−GSO_3^-

complex determined to 2.9 Å raises the interesting possibility that very precise interactions with GSH are a prerequisite for efficient LTA_4 binding. In this study, we present pre-steady-state kinetic data as well as data from potentiometric measurements supporting the notion that all three active sites of hLTC4S are able to bind and form a thiolate anion. The formation of the GSH thiolate is not rate-limiting for the overall catalytic formation of LTC_4.

AUTHOR INFORMATION

Corresponding Author

*J.Z.H.: e-mail, jesper.haeggstrom@ki.se; phone, +46-8-52487612; fax, +46-8-7360439. R.M.: e-mail, ralf.morgenstern@ki.se; phone, +46-8-52487574; fax, +46-8-343849.

Funding

This work was supported by grants from the Swedish Research Council (J.Z.H., R.M., and A.R.-M.), CIDaT (Vinnova), the Torsten and Ragnar Söderbergs Foundation, and Atheroremo (201668). J.Z.H. is the recipient of a Distinguished Professor Award from Karolinska Institutet.

ACKNOWLEDGMENTS

We greatly thank the staff of the European synchrotron radiation facility (ESRF) at beamline ID23-2 for technical assistance during data collection as well as Eva Ohlson for technical assistance in the lab.

ABBREVIATIONS

cys-LTs, cysteinyl-leukotrienes; GSH, glutathione; LT, leukotriene; 5-LO, 5-lipoxygenase; LTA_4, 5(*S*)-*trans*-5,6-oxido-7,9-*trans*-11,14-*cis*-eicosatetraenoic acid; LTC_4, 5(*S*)-hydroxy-6(*R*)-*S*-glutathionyl-7,9-*trans*-11,14-*cis*-eicosatetraenoic acid; LTD_4, 5(*S*)-hydroxy-6(*R*)-*S*-cysteinylglycyl-7,9-*trans*-11,14-*cis*-eicosatetraenoic acid; LTE_4, 5(*S*)-hydroxy-6(*R*)-*S*-cysteinyl-7,9-*trans*-11,14-*cis*-eicosatetraenoic acid; hLTC4S, human leukotriene C_4 synthase; MGST, microsomal GSH transferase; MAPEG, membrane-associated proteins in eicosanoid and glutathione metabolism; mPGES1, microsomal PGE-synthase 1; IMAC, immobilized metal affinity chromatography; glutathione sulfonic acid, (2*S*)-2-amino-5-{[(2*R*)-1-(carboxymethylamino)-1-oxo-3-sulfopropan-2-yl]amino}-5-oxopentanoic acid; rmsd, root-mean-square deviation.

REFERENCES

(1) Samuelsson, B. (1983) Leukotrienes: Mediators of immediate hypersensitivity reactions and inflammation. *Science 220*, 568−575.

(2) Haeggström, J. Z., and Funk, C. D. (2011) Lipoxygenase and leukotriene pathways, biochemistry, biology, and roles in disease. *Chem. Rev. 111*, 5866−5898.

(3) Rinaldo-Matthis, A., and Haeggstrom, J. Z. (2010) Structures and mechanisms of enzymes in the leukotriene cascade. *Biochimie 92*, 676−681.

(4) Drazen, J. M., Israel, E., and O'Byrne, P. M. (1999) Treatment of asthma with drugs modifying the leukotriene pathway. *N. Engl. J. Med. 340*, 197−206.

(5) Martinez Molina, D., Eshaghi, S., and Nordlund, P. (2008) Catalysis within the lipid bilayer-structure and mechanism of the MAPEG family of integral membrane proteins. *Curr. Opin. Struct. Biol. 18*, 442−449.

(6) Ford-Hutchinson, A. W., Gresser, M., and Young, R. N. (1994) 5-Lipoxygenase. *Annu. Rev. Biochem. 63*, 383−417.

(7) Thoren, S., Weinander, R., Saha, S., Jegerschold, C., Pettersson, P. L., Samuelsson, B., Hebert, H., Hamberg, M., Morgenstern, R., and Jakobsson, P. J. (2003) Human microsomal prostaglandin E synthase-1: Purification, functional characterization, and projection structure determination. *J. Biol. Chem. 278*, 22199−22209.

(8) Rinaldo-Matthis, A., Wetterholm, A., Molina, D. M., Holm, J., Niegowski, D., Ohlson, E., Nordlund, P., Morgenstern, R., and Haeggstrom, J. Z. (2010) Arginine 104 is a key catalytic residue in leukotriene C4 synthase. *J. Biol. Chem. 285*, 40771−40776.

(9) Holm, P. J., Bhakat, P., Jegerschold, C., Gyobu, N., Mitsuoka, K., Fujiyoshi, Y., Morgenstern, R., and Hebert, H. (2006) Structural basis for detoxification and oxidative stress protection in membranes. *J. Mol. Biol. 360*, 934−945.

(10) Hammarberg, T., Hamberg, M., Wetterholm, A., Hansson, H., Samuelsson, B., and Haeggström, J. Z. (2009) Mutation of a critical arginine in microsomal prostaglandin E synthase-1 shifts the isomerase activity to a reductase activity that converts prostaglandin H2 into prostaglandin F2α. *J. Biol. Chem. 284*, 301−305.

(11) Jegerschöld, C., Pawelzik, S. C., Purhonen, P., Bhakat, P., Gheorghe, K. R., Gyobu, N., Mitsuoka, K., Morgenstern, R., Jakobsson, P. J., and Hebert, H. (2008) Structural basis for induced formation of the inflammatory mediator prostaglandin E2. *Proc. Natl. Acad. Sci. U.S.A. 105*, 11110−11115.

(12) Uozumi, N., Kume, K., Nagase, T., Nakatani, N., Ishii, S., Tashiro, F., Komagata, Y., Maki, K., Ikuta, K., Ouchi, Y., Miyazaki, J., and Shimizu, T. (1997) Role of cytosolic phospholipase A2 in allergic response and parturition. *Nature 390*, 618−622.

(13) Martinez Molina, D., Wetterholm, A., Kohl, A., McCarthy, A. A., Niegowski, D., Ohlson, E., Hammarberg, T., Eshaghi, S., Haeggström, J. Z., and Nordlund, P. (2007) Structural basis for synthesis of inflammatory mediators by human leukotriene C4 synthase. *Nature 448*, 613−616.

(14) Lowry, O. H., Rosebrough, N. J., Farr, A. L., and Randall, R. J. (1951) Protein measurement with the Folin phenol reagent. *J. Biol. Chem. 193*, 265−275.

(15) Kabsch, W. (1988) Automatic indexing of rotation diffraction patterns. *J. Appl. Crystallogr. 21*, 67−72.

(16) Evans, P. (2006) Scaling and assessment of data quality. *Acta Crystallogr. D62*, 72−82.

(17) Potterton, E., Briggs, P., Turkenburg, M., and Dodson, E. (2003) A graphical user interface to the CCP4 program suite. *Acta Crystallogr. D59*, 1131−1137.

(18) Murshudov, G. N., Vagin, A. A., and Dodson, E. J. (1997) Refinement of macromolecular structures by the maximum-likelihood method. *Acta Crystallogr. D53*, 240−255.

(19) Emsley, P., and Cowtan, K. (2004) Coot: Model-building tools for molecular graphics. *Acta Crystallogr. D60*, 2126−2132.

(20) Graminski, G. F., Kubo, Y., and Armstrong, R. N. (1989) Spectroscopic and kinetic evidence for the thiolate anion of glutathione at the active site of glutathione S-transferase. *Biochemistry 28*, 3562−3568.

(21) Caccuri, A. M., Lo Bello, M., Nuccetelli, M., Nicotra, M., Rossi, P., Antonini, G., Federici, G., and Ricci, G. (1998) Proton release upon glutathione binding to glutathione transferase P1-1: Kinetic analysis of a multistep glutathione binding process. *Biochemistry 37*, 3028−3034.

(22) Davis, I. W., Leaver-Fay, A., Chen, V. B., Block, J. N., Kapral, G. J., Wang, X., Murray, L. W., Arendall, W. B. III, Snoeyink, J., Richardson, J. S., and Richardson, D. C. (2007) MolProbity: All-atom contacts and structure validation for proteins and nucleic acids. *Nucleic Acids Res. 35*, W375−W383.

(23) Armstrong, R. N. (1997) Structure, catalytic mechanism, and evolution of the glutathione transferases. *Chem. Res. Toxicol. 10*, 2−18.

(24) Ago, H., Kanaoka, Y., Irikura, D., Lam, B. K., Shimamura, T., Austen, K. F., and Miyano, M. (2007) Crystal structure of a human membrane protein involved in cysteinyl leukotriene biosynthesis. *Nature 448*, 609−612.

(25) Liu, S., Zhang, P., Ji, X., Johnson, W. W., Gilliland, G. L., and Armstrong, R. N. (1992) Contribution of tyrosine 6 to the catalytic mechanism of isoenzyme 3-3 of glutathione S-transferase. *J. Biol. Chem. 267*, 4296−4299.

(26) Alander, J., Lengqvist, J., Holm, P. J., Svensson, R., Gerbaux, P., Heuvel, R. H., Hebert, H., Griffiths, W. J., Armstrong, R. N., and

Morgenstern, R. (2009) Microsomal glutathione transferase 1 exhibits one-third-of-the-sites-reactivity towards glutathione. *Arch. Biochem. Biophys. 487*, 42−48.
(27) Morgenstern, R., Svensson, R., Bernat, B. A., and Armstrong, R. N. (2001) Kinetic analysis of the slow ionization of glutathione by microsomal glutathione transferase MGST1. *Biochemistry 40*, 3378−3384.
(28) Fersht, A. (1999) *Structure and Mechanism in Protein Science: A Guide to Enzyme Catalysis and Protein Folding*, W. H. Freeman and Co., New York.
(29) Patskovsky, Y., Patskovska, L., Almo, S. C., and Listowsky, I. (2006) Transition state model and mechanism of nucleophilic aromatic substitution reactions catalyzed by human glutathione S-transferase M1a-1a. *Biochemistry 45*, 3852−3862.
(30) Widersten, M., Bjornestedt, R., and Mannervik, B. (1996) Involvement of the carboxyl groups of glutathione in the catalytic mechanism of human glutathione transferase A1-1. *Biochemistry 35*, 7731−7742.
(31) Dirr, H., Reinemer, P., and Huber, R. (1994) X-ray crystal structures of cytosolic glutathione S-transferases. Implications for protein architecture, substrate recognition and catalytic function. *Eur. J. Biochem. 220*, 645−661.
(32) Dourado, D. F., Fernandes, P. A., Mannervik, B., and Ramos, M. J. (2008) Glutathione transferase: New model for glutathione activation. *Chemistry 14*, 9591−9598.
(33) Patskovsky, Y. V., Patskovska, L. N., and Listowsky, I. (2000) The enhanced affinity for thiolate anion and activation of enzyme-bound glutathione is governed by an arginine residue of human mu class glutathione S-transferases. *J. Biol. Chem. 275*, 3296−3304.
(34) Bjornestedt, R., Tardioli, S., and Mannervik, B. (1995) The high activity of rat glutathione transferase 8-8 with alkene substrates is dependent on a glycine residue in the active site. *J. Biol. Chem. 270*, 29705−29709.
(35) Prage, E. B., Pawelzik, S. C., Busenlehner, L. S., Kim, K., Morgenstern, R., Jakobsson, P. J., and Armstrong, R. N. (2011) Location of inhibitor binding sites in the human inducible prostaglandin E synthase, MPGES1. *Biochemistry 50*, 7684−7693.
(36) Nishida, M., Harada, S., Noguchi, S., Satow, Y., Inoue, H., and Takahashi, K. (1998) Three-dimensional structure of *Escherichia coli* glutathione S-transferase complexed with glutathione sulfonate: Catalytic roles of Cys10 and His106. *J. Mol. Biol. 281*, 135−147.
(37) Gupta, N., Greeser, M. J., and Ford-Hutchinson, A. W. (1999) A random rapid equilibrium mechanism for leukotriene C4 synthase. *Adv. Exp. Med. Biol. 469*, 327−332.